Title
TEMPERATURE-DEPENDENT ULTRAVIOLET ABSORPTION SPECTRUM FOR N2O5

Authors
Yao, F.
Wilson, I.
Johnston, H.

Publication Date
1982-03-01

LBL-14340
Preprint

Lawrence Berkeley Laboratory
UNIVERSITY OF CALIFORNIA

Materials & Molecular
Research Division

Submitted to the Journal of Physical Chemistry

TEMPERATURE-DEPENDENT ULTRAVIOLET ABSORPTION SPECTRUM FOR N_2O_5

Francis Yao, Ivan Wilson, and Harold Johnston

March 1982

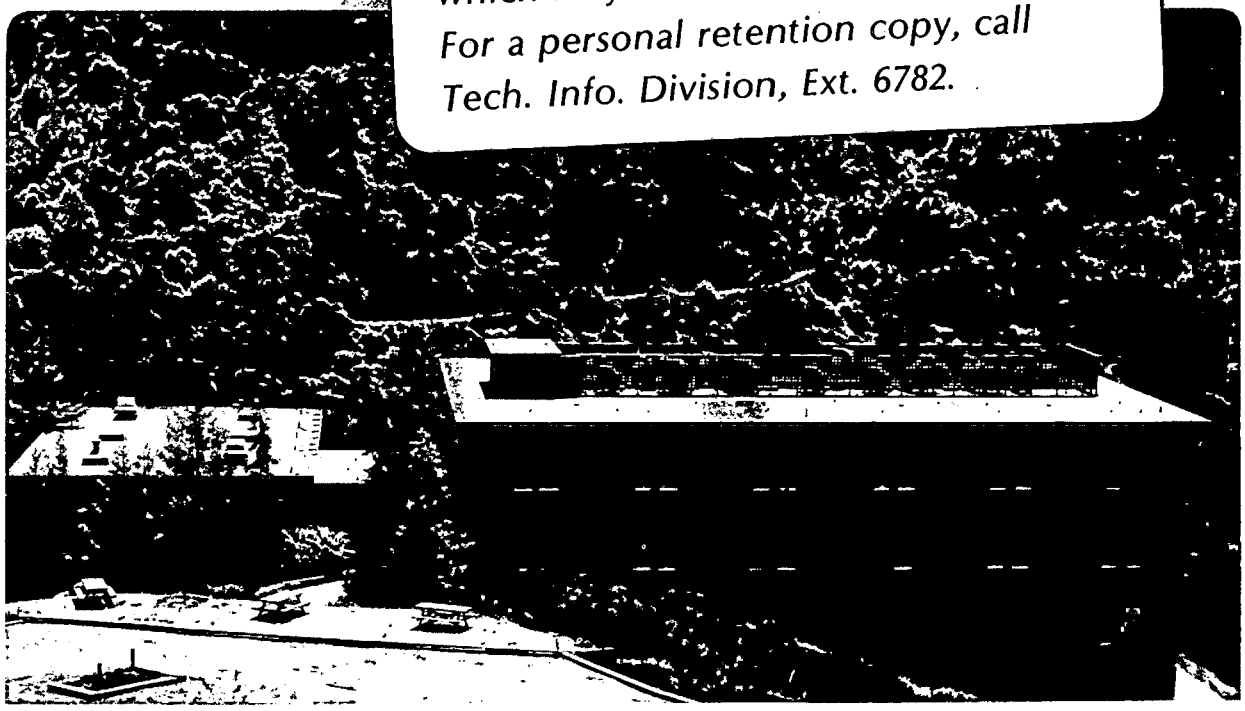

Prepared for the U.S. Department of Energy under Contract DE-AC03-76SF00098

DISCLAIMER

Temperature-Dependent Ultraviolet Absorption Spectrum for N_2O_5

Francis Yao, Ivan Wilson,† and Harold Johnston*

Department of Chemistry, University of California

and

Materials and Molecular Research Division,

Lawrence Berkeley Laboratory,

Berkeley, California 94720

Abstract

The ultraviolet absorption cross-sections for N_2O_5 are presented for wavelengths between 200 and 380 nm and for temperatures between 223 and 300 K. The absorption spectrum above 290 nm shows a pronounced temperature dependence.

This work was supported by the Director, Office of Energy Research, Office of Basic Energy Sciences, Chemical Sciences Division of the U.S. Department of Energy under Contract Number DE-AC03-76SF00098. This manuscript was printed from originals provided by the authors.

†Present address: Department of Chemistry, Monash University, Wellington Road, Clayton, Victoria, Australia 3168.

Introduction

Di-nitrogen pentoxide, N_2O_5, may be a significant reservoir for stratospheric nitrogen oxides, especially at night and in the polar night. The room-temperature ultraviolet cross-sections for N_2O_5 were reported between 285 and 380 nm by Jones and Wulf,[1] between 210 and 290 nm by Johnston and Graham,[2] and between 205 and 310 nm by Graham.[3] This study reinvestigated the absorption cross-sections

$$\sigma = (\ell n I_o/I)(N_5 L)^{-1} \qquad (1)$$

where N_5 is the concentration of N_2O_5 in molecules cm^{-3} and L is the optical path in cm, as a function of temperature and wavelength. Since the primary quantum yield for N_2O_5 photolysis appears to be unity and the primary products appear to be $2NO_2 + O(^3P)$,[4,5] data now exist to permit evaluation of photolysis rate coefficients in the stratosphere.

It is difficult to measure the ultraviolet absorption cross-sections of N_2O_5. The molecule undergoes a slow irreversible decomposition (primarily homogeneous above room temperature and primarily heterogeneous below 0°C)

$$2N_2O_5 \rightarrow 4NO_2 + O_2 \qquad . \qquad (2)$$

The nitrogen dioxide thus produced rapidly reversibly associates to form di-nitrogen tetroxide

$$N_2O_4 \rightleftarrows 2NO_2 \qquad . \qquad (3)$$

Di-nitrogen pentoxide reacts strongly with surface-adsorbed water to form nitric acid

$$N_2O_5 + H_2O \rightarrow 2HNO_3 \quad . \tag{4}$$

As usually prepared, N_2O_5 contains a few percent nitric acid. The by-products NO_2 and N_2O_4 may be suppressed by addition of ozone

$$2NO_2 + O_3 \rightarrow N_2O_5 + O_2 \tag{5}$$

but the ozone is fairly rapidly destroyed by N_2O_5 catalysis

$$2O_3 + N_2O_5 \rightarrow 3O_2 + N_2O_5 \quad . \tag{6}$$

All of these by-products, NO_2, N_2O_4, HNO_3, and O_3, absorb strongly somewhere in the near ultraviolet and set up time-dependent interferences with the quantity of interest.

The first successful measurement of N_2O_5 cross-sections was by Jones and Wulf.[1] They added ozone to N_2O_5, letting (5) suppress NO_2 and N_2O_4 and letting (6) smoothly remove the added ozone. They repeatedly photographed the ultraviolet spectrum between 290 and 400 nm, and they selected for the N_2O_5 spectrum the one where ozone was essentially all gone and where NO_2 had not yet built up. In a steady-state flowing long-path single-pass experiment, Johnston and Graham[2] scanned the spectrum of N_2O_5 and ozone, and subtracted the contribution of ozone. In a similar long-path cell Graham[3] measured the concentration of N_2O_5, HNO_3, and NO_2 by infrared absorption in a flowing system, switched optics to measure the ultraviolet spectrum, and applied corrections for HNO_3 and NO_2 (N_2O_4 was negligible in this system).

Experimental

In this study, the ultraviolet absorption spectrum of N_2O_5 was obtained between 200 and 380 nm and between 220 and 300 K. Two series of experiments were carried out, one series in 1978 and one in 1981. Each series used a Cary 118C double-beam spectrophotometer and two cells:[6] (1) One, constructed of silica, had an optical path of 10 cm, and it consisted of three fused concentric cylinders. The N_2O_5 gas was in the central cell, a circulating thermostated fluid surrounded the central cell except at the ends, and this system was surrounded by an insulating evacuated outer cell. This cell was mounted in the regular sample compartment of the Cary 118C. (2) By means of a set of mirrors the sample beam of the spectrophotometer was sent through a window into a stainless steel tube 8 cm in diameter and 160 cm long. A mirror at the far end returned the beam, so that the cell was double passed with optical path of 296 cm. The cell was encircled with a coiled copper tube containing a circulating thermostated fluid, and both coil and tube were submerged in a bath of methanol, which was heavily insulated on the outside. Temperature was measured by two thermometers inserted in the methanol bath. The N_2O_5 was made by reacting NO_2 with excess ozone, reaction (5), and it was frozen out at -78°C.

In the first series the spectra were recorded each nm through a 12-bit analog-to-digital converter and stored in a multi-channel storage computer. The concentration of NO_2 was measured from absorption at 400 nm, and the optical-densities at all wavelengths were calculated from that at 400 nm using the temperature-dependent cross-sections reported by Bass *et al.*[7] The N_2O_4 concentration was calculated from

the observed NO_2 and the equilibrium constant for reaction (2),[8] and the corresponding optical density was calculated from N_2O_4 cross-sections also reported by Bass et al.[7] The corrections were scaled and subtracted from the observed optical density in the laboratory minicomputer. Multiple scans at one temperature were averaged.

After the first series was completed, it was recognized that Bass' cross-sections for NO_2 were obtained with much higher resolution than that of the Cary 118C spectrophotometer. Above about 340 nm, the NO_2 cross sections are 100 to 1000 fold larger than the N_2O_5 cross sections, and the correction for NO_2 is a large fraction of the observed signal. The mis-match in resolution between the instrument used here and that used by Bass appeared to introduce a large error in these results, especially above 330 nm. At wavelengths below 220 nm, the cross-section for HNO_3 rapidly increases to large values,[9] and this series had no method for correction for HNO_3. The second series was designed to apply appropriate corrections for NO_2 and for HNO_3.

Experiments in the second series were made at static settings of the spectrometer wavelength drive at each 5 nm position between 400 and 200 nm, and the optical density was written down from the illuminated digital meter. At each temperature and at each wavelength calibrations were made to obtain the cross-sections for NO_2 and N_2O_4 with the same spectral resolution used for N_2O_5 (0.3 mm slits on the Cary 118C, which corresponds to 0.9 nm at 300 nm and 0.18 nm at 200 nm). The methods used are explained in terms of the symbols and definitions in Table 1.

During a calibration the total concentration of NO_2 plus N_2O_4 was measured by a Texas Instruments quartz-spiral manometer

$$N = N_2 + N_4 = N_2 + N_2^2/K \tag{7}$$

The observed optical density is likewise the sum of the two components

$$D = D_2 + D_4 = \sigma_2 L N_2 + \sigma_4 L N_4 \quad . \tag{8}$$

At 400 nm there is no absorption by N_2O_4 so that the optical density there is a measure of the species NO_2

$$N_2 = D^o/\sigma_2{}^o L \tag{9}$$

For a series of experiments at 400 nm the ratio of observed N and observed D^o is

$$\frac{N}{D^o} = \frac{1}{\sigma_2{}^o L} + \frac{1}{K(\sigma_2{}^o L)^2} D^o \quad . \tag{10}$$

A plot of N/D^o against D^o gives the NO_2 cross-section at 400 nm, $\sigma_2{}^o$, from the intercept, and the equilibrium constant K for reaction (3) from the slope. The temperature was read by two calibrated thermometers inserted at the entrance and at the exit of the body of insulated, circulating fluid around the cell. At the end of the experiments, these thermometers were found to require significant stem corrections, and they overestimated the temperature of the body of the fluid by as much as 5°C at -50°C. The temperature used in interpreting the data is that derived from the measured equilibrium constant and its temperature dependence (Table 1). For a series of calibration experiments each spanning the range 400 to 200 nm, the ratio of observed optical density D and that observed at 400 nm is

$$\frac{D}{D^o} = \frac{\sigma_2}{\sigma_2{}^o} + \frac{\sigma_4}{KL(\sigma_2{}^o)^2} D^o \tag{11}$$

$$= i + sD^o \quad . \tag{12}$$

From (10) the terms σ_2^o and K are already known, so that a plot of D/D^o against D^o at each wavelength yields the NO_2 cross-section σ_2 from the intercept $\underline{i}$ and the N_2O_4 cross-section σ_4 from the slope $\underline{s}$, which are thus obtained at the same temperature, wavelength, and spectral resolution as those used for the studies with N_2O_5.

During experiments with N_2O_5, where some HNO_3 was present, the total pressure yields the total number of gas-phase species

$$N = N_2 + N_4 + N_5 + N_A \tag{13}$$

and the observed optical density is

$$D = D_2 + D_4 + D_5 + D_A \quad . \tag{14}$$

At wavelengths above 240 nm where the cross-section of HNO_3 is small, the cross-section for N_2O_5 is

$$\sigma_5 = [D - iD^o - s(D^o)^2]/LN_5 \tag{15}$$

where D is the total optical density at any wavelength λ, D^o is the optical density at 400 nm in the same mixture, and $\underline{i}$ and $\underline{s}$ are evaluated in the calibration experiments. If HNO_3 were absent, the concentration of N_2O_5 could be evaluated from the "total-pressure method"

$$N_5 = N - \frac{D^o}{\sigma_2^o L} - \left(\frac{D^o}{\sigma_2^o L}\right)^2 \frac{1}{K} \quad . \tag{16}$$

The effect of nitric acid was eliminated by use of the "kinetic method" described below.

As N_2O_5 undergoes irreversible decomposition (2), there is a stoichiometric relation between change of N_2O_5 and reaction products

$$-\frac{dN_5}{dt} = \frac{1}{2}\frac{dN_2}{dt} + \frac{dN_4}{dt} \tag{17}$$

and the relation (3) between NO_2 and N_2O_4 gives

$$\frac{dN_4}{dt} = 2N_2\frac{dN_2}{dt} \tag{18}$$

The change in observed optical density (14) is

$$\frac{1}{L}\frac{dD}{dt} = \sigma_2\frac{dN_2}{dt} + \sigma_4\frac{dN_4}{dt} + \sigma_5\frac{dN_5}{dt} + \sigma_A\frac{dN_A}{dt} \tag{19}$$

Since HNO_3 does not change in reaction (2) the last term in (19) is zero [provided the apparatus had been essentially stabilized with respect to reaction (4) before the series began, which was the case during these runs]. Equations (17)-(19) can be combined

$$\int_o^t dD = \frac{\left(\sigma_2 - \frac{1}{2}\sigma_5\right)}{\sigma_2^o}\int_o^t dD^o + \frac{2\left(\sigma_4 - \sigma_5\right)}{K\left(\sigma_2^o\right)^2 L}\int_o^t D^o dD^o \tag{20}$$

which can be integrated to give

$$\frac{D - D_o}{D^o - D_o^o} = \frac{\left(\sigma_2 - \frac{\sigma_5}{2}\right)}{\sigma_2^o} + \frac{\left(\sigma_4 - \sigma_5\right)\left(D^o + D_o^o\right)}{K\left(\sigma_2^o\right)^2 L} \tag{21}$$

where subscript zero refers to initial time and superscript zero refers to 400 nm. This equation can be solved for the N_2O_5 cross-section

$$\sigma_5 = \frac{2\sigma_2^{\,o}\left[1 + s\left(D^o + D_o^{\,o}\right) - \dfrac{D - D_o}{D^o - D_o^{\,o}}\right]}{\left[1 + \dfrac{2\sigma_2^{\,o} s}{\sigma_4}\left(D^o + D_o^{\,o}\right)\right]} \quad . \qquad (22)$$

The kinetic method balances the change of N_2O_5 against the change of NO_2 and N_2O_4. It is most suitable at wavelengths where the N_2O_5 cross-section is equal to or greater than that of NO_2, that is below 280 nm. At longer wavelengths the expression involves the small difference between large numbers, but below about 280 nm the term $(D - D_o)/(D^o - D_o^{\,o})$ is negative so that all terms in the numerator are positive, and the method has good stability. For a given run, the kinetic method applied below 280 nm yielded the actual concentration of N_2O_5, which could then be substituted in (15) to give σ_5 at wavelengths above 280 nm. This combination of the kinetic method and total pressure method eliminated the effect of HNO_3 both in its contribution to optical density and to total pressure.

In carrying out the kinetic method, a small amount of ozone was usually added, which converted essentially all NO_2 and N_2O_4 to N_2O_5 (5). Ozone is catalytically decomposed by N_2O_5 (6), and its concentration smoothly fell to zero. After that, the kinetic method followed the simultaneous decay of N_2O_5 and build-up of NO_2 and N_2O_4 (2,3).

Results

Cross-sections for N_2O_5 as obtained in the first series are plotted as dots in Fig. 1. The temperature was 273 K and the wavelength range was 230 to 380 nm. The method shows good reproducibility between 230

and 330 nm, but the scatter is large above about 340 nm. Much of this scatter can be ascribed to the large relative correction for NO_2 in this wavelength region and for the mis-match in resolution between this experiment and that of Bass et al.,[7] whose NO_2 spectra were used to make the NO_2 corrections.

Averaged results of the second series at 276 K are included at 10 nm intervals in Fig. 1. The central symbol at each interval represents results in the large stainless-steel cell with 296 cm path length, the height of the symbol represents one standard deviation (not the standard deviation of the mean), and approximately 10 to 20 points are averaged at each wavelength. The symbol to the left at each 10 nm interval represents data taken in the 10 cm silica cell by the kinetic method (about 5 points were averaged at each wavelength), and the symbol to the right represents data taken in the 10 cm silica cell by the total-pressure method (about 10 points were averaged at each wavelength). Results were obtained at 5 nm intervals, but to avoid crowding the figure only results on even 10 nm intervals are shown here. At this temperature (273-276 K) the two series of data are in satisfactory agreement. The data in the first series show a large scatter at long wavelengths above about 350 nm. The kinetic method in the second series disagrees with the other methods at 290 and 300 nm, and it was not stable above this wavelength.

On expanded scales, the first-series results at various temperatures are given in Fig. 2: A, 230-280 nm; B, 280-340 nm. Between 310 and 340 nm, the N_2O_5 cross-sections show a pronounced temperature effect, decreasing with decreasing temperature. At long wavelengths the noise in the data is such that it was not possible to establish the quantitative

aspects of the temperature coefficient. Below 280 nm, there appears to be little or no temperature dependence of the cross-sections. There is as great a spread between results of 273 and 266 K, which are virtually the same temperature for these purposes, as there is between 273 and 234 K. One series of runs was made between 230 and 290 nm at 216 K, which was about 20 percent lower than the results at 266 K. At the time the experiments were taken, there was evidence that some N_2O_5 had condensed out on the walls of the cell; and data at 223 K in the second series established that the 216 K data of the first series were invalid. These data at 216 K have been omitted from this report.

The main emphasis in the second series was to take data suitable for establishing the temperature dependence of the cross-sections between 300-380 nm. At each wavelength, the cross-sections gave a good straight line on an Arrhenius plot (which is a speacilized way of expressing the Boltzmann relation)

$$\ell n\sigma = \ell nA - E/T \quad . \tag{23}$$

The average values of the N_2O_5 cross-sections as obtained in the second series are plotted at 10 nm intervals according to (23) in Fig. 3 between 223 and 300 K and between 290 and 380 nm. Alternate sets of data are presented as open and as filled circles or squares so that there is no uncertainty as to which set a given point belongs. From Fig. 3 it can be seen that the slope E increases with increase in wavelength, and it was found that the coefficients E changed linearly with wavelength between 300 and 380 nm. On this basis all data points in the second series (290-380 nm, 241-300 K) were simultaneously fit by least squares to the two-variable, three-parameter relation

$$\ell n\sigma = A + B(1000/T) + C(\lambda/T) \quad . \quad (24)$$

The numerical values of these parameters are conveniently expressed as

$$\ell n\sigma = 0.432537 + (4.72848 - 0.0171269\ \lambda)(1000/T) \quad (25)$$

where σ is in units of 10^{-19} cm^2 and λ is wavelength in nm. (Extra digits are retained in this empirical formula to guarantee the significance of the differences; the final result is significant to only 2 figures.) All of the lines in Fig. 3 are calculated from (25), and this simple single expression satisfactorily represents all of the data. The runs at 223 K (squares in Fig. 3) were not included in the least-squares fit to give (25), because data at this temperature did not give a fully satisfactory set of N_2O_4 cross-sections in the calibration experiments (7 to 12). Even so, these points are satisfactorily predicted by (25).

Although there is some hint of temperature effect on the N_2O_5 cross-section below 280 nm, Fig. 2, the trend is so slight that all data points from 223 to 300 K of both series one and series two were averaged every 5 nm between 200 and 280 nm, and these data are given in Table 2. Below 230 nm these results are exclusively from the second series, and they are based on the kinetic method, which tends to eliminate the perturbing effect of HNO_3 on the results.

Previous measurements[1-3] of the N_2O_5 cross-sections were done at 298 or 300 K. The line in Fig. 4 is based on the average observed points (Table 2) from 200 to 280 nm and the points calculated (25) from 285 to 380 at 300 K. The circles represent Graham's[3] values and the triangles represent the results of Jones and Wulf.[1] The present results are fairly well parallel to those of Graham between 210 and 310 nm but are about 10 percent higher. The present results are not strictly

parallel to and average about 30 percent higher than those of Jones and Wulf between 290 and 380 nm. In view of the difficulty in handling N_2O_5 and its decomposition products, Fig. 4 shows reasonably good agreement between these and other results at 300 K.

Discussion

The explanation for the increase with temperature in cross-section at long wavelengths is that thermal excitation of vibrational and rotational states in the ground electronic state of the molecule makes available low energy, long wavelength transitions. The population of such states is expected to parallel the Boltzmann factor, $\exp(-\varepsilon/kT)$, and the linear relation shown in Fig. 3 is reasonable. Such an effect may be expected on the long-wavelength side of an absorption peak, but regions near the maximum of the absorption peak usually show little or no effect of modest temperature changes.

The decrease of cross section with decrease of temperature largely occurs above 300 nm. For considerations of atmospheric photochemistry, this is the wavelength region where solar radiation penetrates to the troposphere and to the ground. Thus the temperature dependence of the N_2O_5 cross-section may be of some importance to the low-temperature upper troposphere and lower stratosphere.

Acknowledgment

This work was supported by the Director, Office of Energy Research, Office of Basic Energy Sciences, Chemical Sciences Division of the U.S. Department of Energy under Contract Number DE-AC03-76SF00098.

References

1. E. L. Jones and O. R. Wulf, J. Chem. Phys. 5, 873 (1937).

2. H. S. Johnston and R. A. Graham, Can. J. Chem. 52, 1415 (1974).

3. R. A. Graham, Ph.D. Thesis, University of California, Berkeley, 1975.

4. P. S. Connell, Ph.D. Thesis, University of California, Berkeley, 1979.

5. Frank Magnotta, Ph.D. Thesis, University of California, Berkeley, 1979.

6. G. S. Selwyn and H. S. Johnston, J. Chem. Phys. 74, 3791 (1981).

7. A. M. Bass, A. E. Leford, Jr. and A. H. Lauber, Journal of Research of the National Bureau of Standards 80A, 143 (1976).

8. V. P. Glushko, V. V. Gurvich, G. A. Bergman, I. V. Veitz, V. A. Medvedev, G. A. Khachkuruzov and V. S. Yungman, Thermodynamic Properties of Individual Substances, High Temperature Institute, State Institute of Applied Chemistry, National Academy of Sciences of the U.S.S.R., Moscow, Volume 1, 1978.

9. H. S. Johnston and R. A. Graham, J. Phys. Chem. 77, 62 (1973).

Table 1. Glossary

Gas concentrations/molecules cm^{-3}

Total, N; NO_2, N_2; N_2O_4, N_4; N_2O_5, N_5; HNO_3, N_A

Optical density: $D = \ell n\ I_o/I$

Cross section/cm^2: $\sigma = D/LN$

σ, σ_2, σ_4, σ_5, σ_A (as for N above)

Properties at 400 nm: D^o, σ^o, $\sigma_2{}^o$

Properties at any wavelength: D, σ, σ_2, etc.

N_2O_4 equilibrium constant[8]

$K = N_2{}^2/N_4 = 1.74 \times 10^{28} \exp(-6661/T)$ molecules cm^{-3}

Table 2. Summary of N_2O_5 cross-sections.

A. λ = 380 to 285 nm. T = 225 to 300 K. Number of runs = 660.

$$\ell n\left(\frac{\sigma}{10^{-19}\ cm^2}\right) = 0.432537 + (4.72848 - 0.0171269\ \lambda)\left(\frac{1000}{T}\right)$$

B. λ = 280 to 200 nm. Little or no temperature dependence, and all data at one temperature averaged together.

$\frac{\lambda}{nm}$	No. of runs	$\frac{\sigma}{10^{-19}\ cm^2}$	$\frac{\lambda}{nm}$	No. of runs	$\frac{\sigma}{10^{-19}\ cm^2}$
280	53	1.17	240	27	6.2
275	50	1.30	235	24	7.7
270	48	1.61	230	17	9.9
265	42	2.0	225	10	14.4
260	40	2.6	220	10	22
255	28	3.2	215	10	37
250	33	4.0	210	8	56
245	29	5.2	205	4	82
			200	4	92

Figure Captions

Figure 1. Comparison of N_2O_5 cross-sections from series one (dots) and series two (bars) at 273-276 K. The dots represent individual cross-section values, and the bars are averages: I, large, long-path, stainless steel cell;], 10 cm silica cell, kinetic method; [, 10 cm silica cell, total pressure method.

Figure 2. Temperature dependence of N_2O_5 cross-sections as obtained in the first series: A, little or no temperature dependence below 280 nm; B, pronounced decrease in cross-sections with decrease of temperature at low temperatures. The noise in these data and the relatively small number of replicate runs make it difficult to establish the quantitative nature of the temperature effect.

Figure 3. Temperature dependence of the N_2O_5 cross-sections as obtained in the second series. The open and filled circles (and also points at the same temperatures obtained every 5 nm) were fit by least squares to (23), and the values of the parameters are given in Table 2 and by (25). All lines are calculated from the three-parameter equation (25). The data at 223 K shown as squares were not included in the evaluation of (25), but these data are satisfactorily predicted by (25).

Figure 4. Comparison of N_2O_5 cross-sections at 298 K as found by this study (the line) and as found by Graham and Johnston (circles) and by Jones and Wulf (triangles).

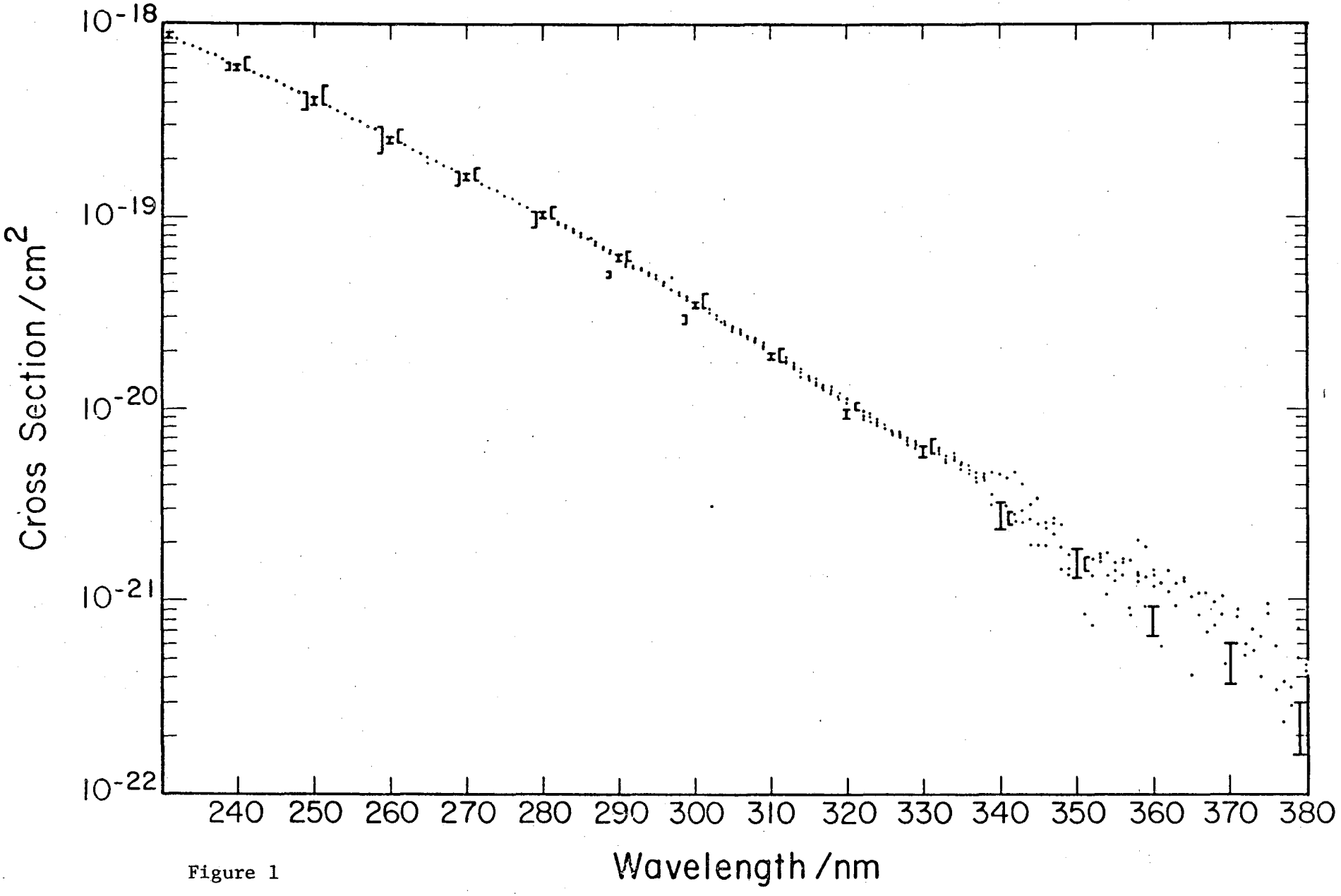
10-18
10-19
10-20
10-21
10-22
Cross Section /cm2
240 250 260 270 280 290 300 310 320 330 340 350 360 370 380
Wavelength /nm

Figure 1

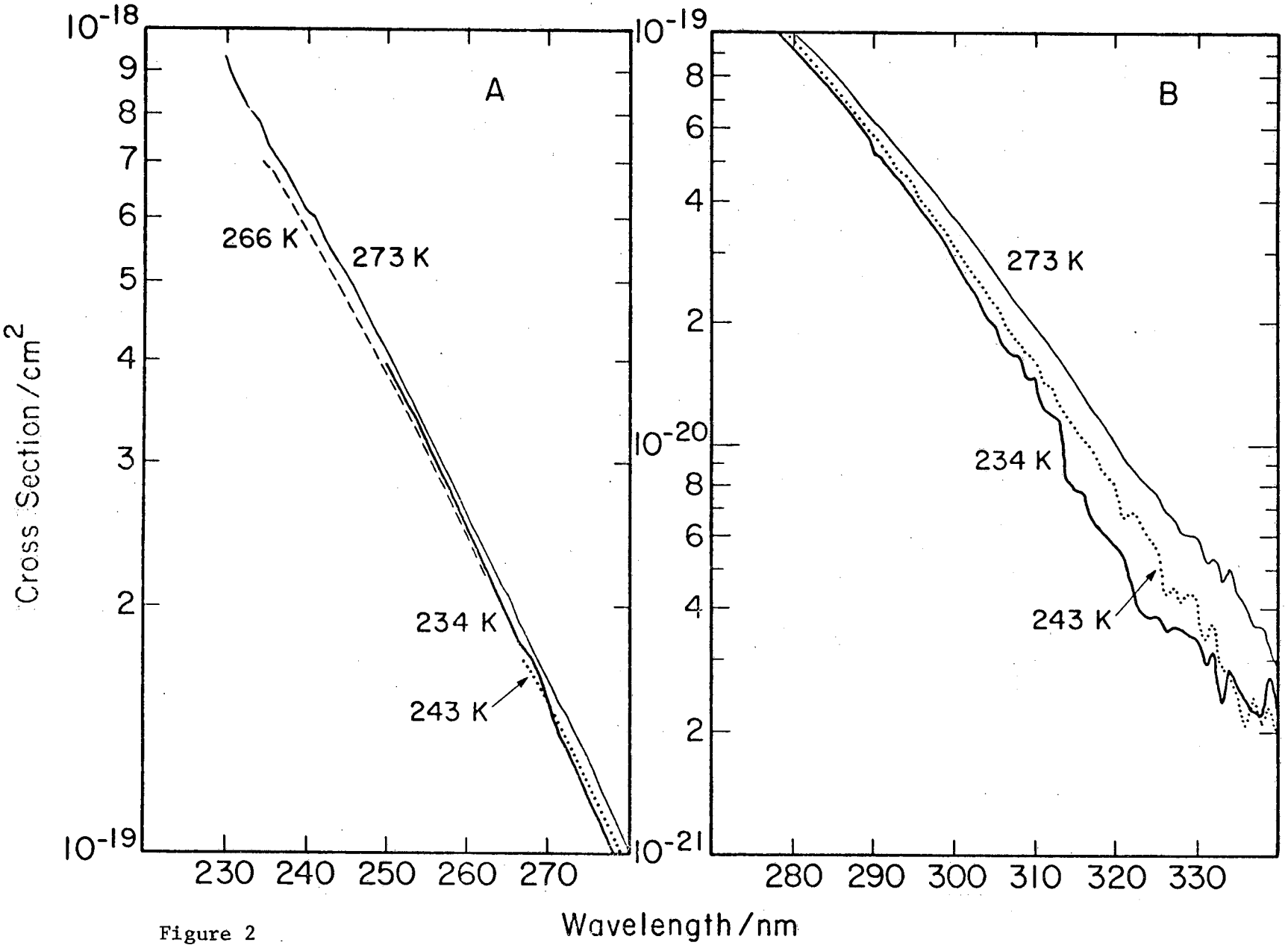
Cross Section/cm^2
10^{-18}
9
8
7
6
5
4
3
2
10^{-19}
A
266 K
273 K
234 K
243 K
230 240 250 260 270
10^{-19}
8
6
4
2
10^{-20}
8
6
4
2
10^{-21}
B
273 K
234 K
243 K
280 290 300 310 320 330
Wavelength/nm

Figure 2

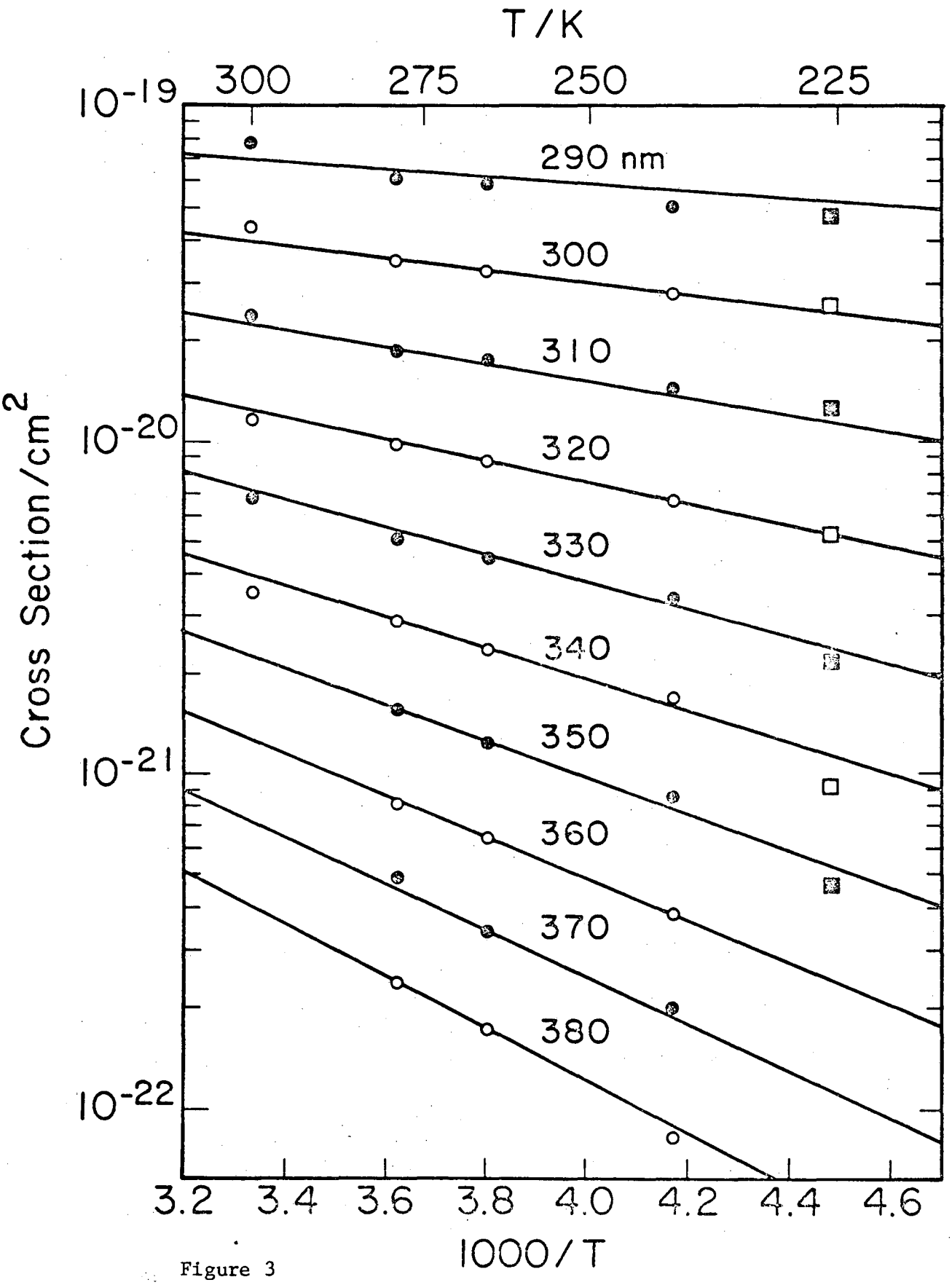
T/K
300
275
250
225
10-19
10-20
10-21
10-22
Cross Section/cm2
290 nm
300
310
320
330
340
350
360
370
380
3.2
3.4
3.6
3.8
4.0
4.2
4.4
4.6
1000/T

Figure 3

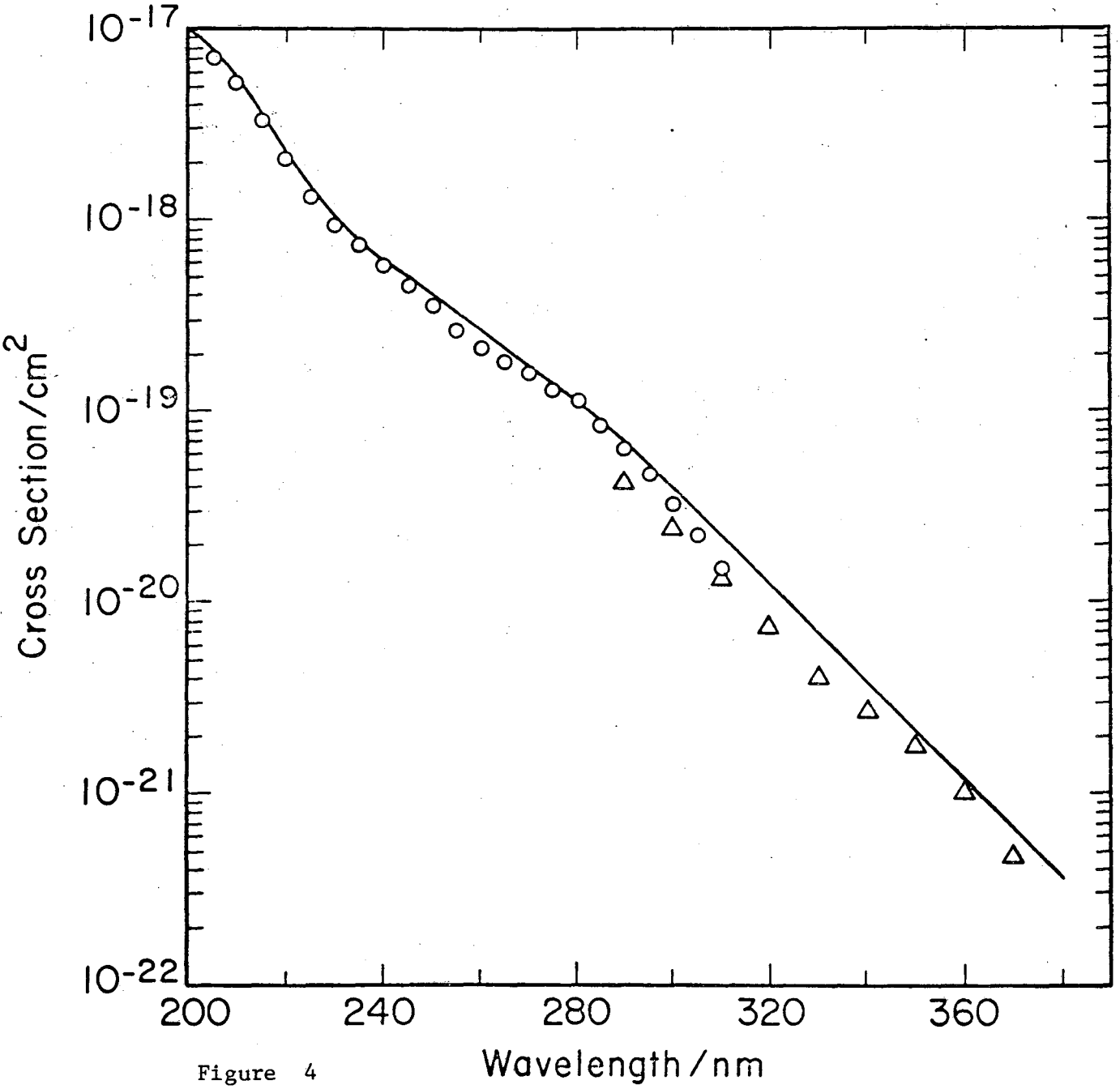
10-17
10-18
10-19
10-20
10-21
10-22
Cross Section/cm2
200
240
280
320
360
Wavelength/nm

Figure 4

TECHNICAL INFORMATION DEPARTMENT
LAWRENCE BERKELEY LABORATORY
UNIVERSITY OF CALIFORNIA
BERKELEY, CALIFORNIA 94720